

Solvation Structure and Transport of Acidic Protons in Ionic Liquids: A First-principles Simulation Study

Mario G. Del Pópolo,^{*,†} Jorge Kohanoff,[‡] and Ruth M. Lynden-Bell^{†,‡}

Atomistic Simulation Centre, School of Mathematics and Physics, Queen's University Belfast, BT7 1NN, U.K., and University Chemical Laboratory, Lensfield Road, Cambridge University, Cambridge CB2 1EW, U.K.

Received: January 12, 2006; In Final Form: March 15, 2006

Ab initio simulations of a single molecule of HCl in liquid dimethyl imidazolium chloride [dmim][Cl] show that the acidic proton exists as a symmetric, linear ClHCl[−] species. Details of the solvation structure around this molecule are given. The proton-transfer process was investigated by applying a force along the antisymmetric stretch coordinate until the molecule broke. Changes in the free energy and local solvation structure during this process were investigated. In the reaction mechanism identified, a free chloride approaches the proton from the side. As the original ClHCl[−] distorts and the incoming chloride forms a new bond to the proton, one of the original chlorine atoms is expelled and a new linear molecule is formed.

1. Introduction

Room temperature ionic liquids (ILs) are fluids composed solely of ions that usually melt at temperatures below 100 °C.^{1,2} The possibility of combining different cations and anions results in a wide variety of ILs which are of interest both for physicochemical studies and for industrial applications.

In contrast with their inorganic counterparts, the fluidity of ILs at ambient temperature permits their use as solvents for chemical reactions, allowing one to explore the effects of purely ionic environments on chemical reactivity.^{1,2} Ions can affect the course of a chemical reaction in different ways, ranging from the solvation of the reaction complex, to the time scale of the ions' dynamical response to changes in the charge distribution of the reactants. A further possibility involves the active participation of the solvent in the chemical process. In particular, hydrogen- and proton-transfer reactions are likely to be very sensitive to an ionic environment due to the hydrogen-bond acceptor ability of most anions.

Given the ubiquitous nature of acid–base processes in solution (i.e., acid–base catalysis), describing the events that follow the addition of a Brønsted acid to a molten salt is a topic of particular relevance. In particular, what is aimed at is a description of the energetic and the solvation structure of acidic protons in ILs, how easily they are released by the conjugated base, and how that depends on the solvent nucleophilicity. It is also important to understand the transport mechanism of acidic protons in the solution.

From a technological point of view, understanding proton transport in molten salts would be insightful for the design of new proton-conducting media for fuel cells and other electrochemical devices.³ For example, the boiling point of water limits the use of aqueous solutions in the manufacture of high-temperature fuel cells. Certain ionic liquids have been proposed as an alternative to cover such deficiency, with the additional benefits of a high thermal stability, wide electrochemical window, and good ionic conductivity.^{4–6}

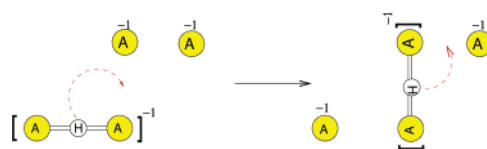


Figure 1. Sketch of a possible proton “hopping” mechanism in molten salts. Anions (A[−]) are used as the donor and acceptor sites. The interaction between the acidic hydrogen (H) and the anions can be of variable strength, favoring in some cases the formation of a stable dianion, AHA[−].

However, to be useful for fuel cells, the ionic liquid has to conduct protons. Several mechanisms have already been suggested. In some cases, the hydrogen carriers are protonated anions or cations, as seems to occur in the “protic” ILs reported by Yoshizawa et al.⁵ There, hydrogen-bonded dianions, like FHF[−] or ClHCl[−], and the protonated cations act as the proton-carrying species. In other systems, where a protic ionic liquid is doped with molecules containing proton acceptor sites, protons can move both by hopping between donor and acceptor molecules or as an integral part of the protonated acceptor molecule. Noda et al. have demonstrated the existence of proton hopping in acid–base ILs doped with amines.⁶ Another possible mechanism involves the participation of the IL anions as donor and acceptor sites, as sketched in Figure 1.

In general, the dominant proton transport mechanism in molten salts will depend on the details of each particular system and will result from a balance between the chemical forces that bind the proton to anions or cations, the viscosity of the fluid at the working temperature, the presence of dopants, and so forth.

Ab initio molecular dynamics simulations, in which the electrons are treated quantum mechanically, provide a good description of processes involving electronic polarization, charge transfer, and the formation and breaking of chemical bonds. These effects are particularly important in the description of the solvation and mobility of acidic protons in solution. As a prototype of an acid–base reaction in ILs, we study the addition of the Brønsted acid HCl to dimethylimidazolium chloride ([dmim][Cl]), whose formula is shown in Figure 2. Our simulations, based on density functional theory (DFT), show

* To whom correspondence should be addressed. Tel: ++44 (2890) 975327. Fax: ++44 (2890) 975359. E-mail: m.del-popolo@qub.ac.uk.

[†] Queen's University Belfast.

[‡] Cambridge University.

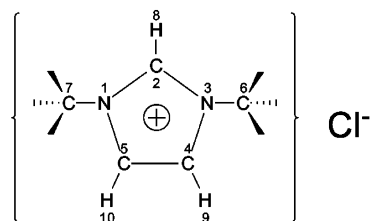


Figure 2. Dimethylimidazolium chloride ([dmim][Cl]).

the immediate formation of a stable molecule of hydrogen dichloride, ClHCl^- . We first perform an equilibrium simulation to find the structure of this anion and the way it is embedded into the structure of the solvent. Then we study the results of forcing one of the $\text{H}-\text{Cl}$ bonds in ClHCl^- to break. This results in the exchange of one of the Cl atoms with a neighboring Cl^- belonging to the solvent to form a new ClHCl^- ion (see Figure 1). Such a process results in an effective hopping of the hydrogen atom. The most plausible reaction mechanism is discussed in terms of the change in some structural parameters involving the reacting atoms and their environment.

2. Computational Details

All the calculations were performed with the SIESTA code,⁷ which is based on density functional theory. In SIESTA, the core electrons are replaced by norm-conserving pseudopotentials and the electronic wave functions of the valence electrons are expanded in a nonorthogonal basis set of atom-centered orbitals. These orbitals are the solution of the pseudoatomic problem, with the additional condition that they exactly vanish at a finite cutoff radius. This condition results in an energy shift of the eigenvalues with respect to the isolated pseudoatoms (infinite radius).

In the present case, the energy shift was set to 50 meV, while an energy cutoff of 200 Ry for the periodic Coulombic sums gave properties converged to acceptable values for a reasonable computational cost. The generalized gradient approximation (GGA), proposed by Perdew, Burke, and Ernzerhof,⁸ was used for the exchange-correlation term of the energy functional, and the pseudopotentials were generated according to the prescription of Troullier and Martins.⁹ The former settings are the same as those in our earlier simulations of pure [dmim][Cl], as reported in ref 10.

All the calculations used FCC periodic boundary conditions (with a dodecahedral repeated MD cell¹¹), to model bulk behavior with a limited number of molecules. Six independent systems, consisting of eight [dmim][Cl] ion pairs plus a single HCl molecule, were each equilibrated for 4 ns using classical potentials. For the ions, the force-field chosen was that of ref 12, while HCl was represented as a flexible diatomic molecule with charges taken from the experimental gas-phase dipole moment and equilibrium distance.¹³ The Lennard-Jones parameters for HCl were the same as those for the hydrogen and chlorine atoms of the solvent.

As described in our previous work,¹⁰ during the classical simulation, the ionic liquid equilibrates to an average structure that is not far from the equilibrium structure corresponding to the DFT simulation. In the present case, that corresponds to a solution of HCl in [dmim][Cl], even though the classical model misrepresents the interaction of HCl with the neighboring ions, the electrostatics is strong enough to generate a hydrogen-bonded pair of the form $\text{Cl}^- \cdots \text{HCl}$. Thus, the classical simulations provide a reasonable starting point for the ab initio trajectories.

[dmim][Cl] is the simplest liquid of the imidazolium series, but unlike most of the series, its melting point is above 373 K. Therefore, the ab initio simulations were run in the NVT ensemble at 450 K (temperature which is in the liquid range), using a Nosé thermostat. The dimensions of the cell were such that the distance between an atom and its nearest lateral image was 13.9 Å (corresponding to a density of 7.267×10^{-2} atoms/Å³ or 9.594×10^2 kg/m³), obtained as an average over a long NPT classical run at 450 K. Hydrogen atoms were replaced by deuterium, and the integration time step was set to 1 fs. Each of the six independent initial configurations was equilibrated for 2 ps, followed by a production run of 4–8 ps. The total simulation time for the sampling of properties was 40 ps. These calculations were used to study the solvation structures of the solute and provided the starting configurations for the simulations used to describe the proton-transfer mechanism.

To force the proton hopping, a reaction coordinate ζ (described in section 4) was chosen. Umbrella sampling calculations were performed by applying a guiding function, $U(\zeta) = 0.7(\text{eV}/\text{\AA}^2)(\zeta - \zeta_i)^2$, to restrain the reaction coordinate to regions around the reference points ζ_i . Calculations were performed for four independent systems, moving toward positive and negative values of ζ . At each value of ζ_i , a new simulation of 2 ps was started from the final configuration obtained at the previous value, ζ_{i-1} . Eighteen values of ζ_i were sampled, leading to a total of 35 ps of simulation time for each system (around 140 ps in total). Several structural features, like coordination numbers and geometry of the reaction complex, were monitored along the reaction coordinate.

3. Structure of ClHCl^- and its Solvation Shell

The addition of an HCl molecule to [dmim][Cl] led to the immediate formation of hydrogen dichloride, ClHCl^- , whose structure stabilized after a few picoseconds. The presence of this anion has been long recognized experimentally, both in liquid and in solid salts containing large cations.^{14–16} Considering that ClHCl^- is one of the simplest hydrogen-bonded systems, much effort has been devoted to its structural and spectroscopic characterization. In the gas phase, experiments¹⁷ and ab initio calculations^{18,19} provided evidence for a linear and symmetric geometry; while in crystals, ClHCl^- is linear but may or may not be centrosymmetric ($D_{\infty h}$ or $C_{\infty v}$) depending on the counterion.^{14,16,20} In any case, the resulting hydrogen bond (~ 100 kJ/mol)¹⁹ is much stronger than that of the neutral dimer $\text{HCl} \cdots \text{HCl}$ (~ 9.5 kJ/mol).²¹

In room-temperature molten salts, ClHCl^- is the principal component in the speciation of the proton in mixtures of chloride- or chloroaluminate ILs and HCl .^{22,23} On the basis of spectroscopic data, Trulove et al. reported a linear symmetric ClHCl^- in [emim][Cl],²³ although neutron diffraction experiments by Trouw and Price seem to indicate an asymmetric molecule.²⁴ In the latter, the asymmetry was attributed to the interaction of ClHCl^- with other components of the mixture, like free Cl^- or the unique hydrogen, H_8 , of the imidazolium ring (see Figure 2).

Given the simplicity of ClHCl^- , deviations from the gas-phase symmetry after dissolving into a condensed phase would induce a noticeable change in the effective potential for the proton motion along the interchlorine line. Such a change would be due to the surrounding ions.

The structure of ClHCl^- can be characterized by the bending angle α and the two hydrogen–chlorine bond lengths, l_1 and l_2 . Figure 3a shows the joint probability distribution $P(l_1, l_2)$ resulting from the simulations, while Figure 3b depicts the

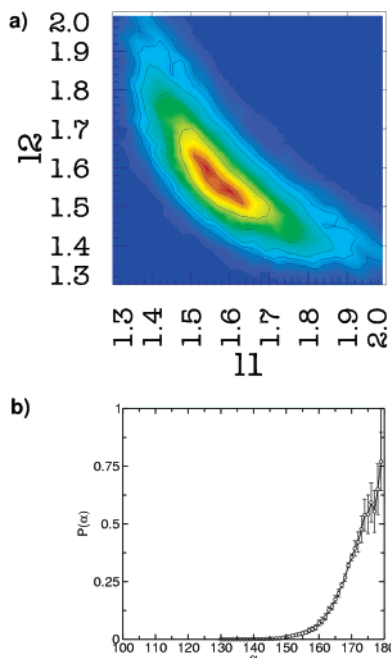


Figure 3. (a) Joint probability distribution $P(l_1, l_2)$, for the two hydrogen–chlorine bond lengths, l_1 and l_2 , in ClHCl^- . (b) Distribution of bending angles, $P(\alpha)$.

distribution of bending angles $P(\alpha)$ weighted with $|\sin(\alpha)|^{-1}$. Both quantities were calculated as an average over six independent trajectories, discarding previous equilibration.

The function $P(l_1, l_2)$ shows a broad maximum near $l_1 = l_2 \sim 1.55$ Å indicating a single well potential or possibly a double well with a very small barrier that the proton can easily cross. We believe that longer runs would show a single well. In any case, the separation between the two alleged minima is small, ~ 0.05 Å, much less than that found in crystals with symmetry breaking. For example, in $[\text{Me}_4\text{N}^+]\text{ClHCl}^-$, $l_1 = 1.36$ Å and $l_2 = 1.85$ Å.¹⁶ The average distance between the two chlorine atoms is 3.11 Å, a value that is similar to the 3.14 Å found in both solid $\text{CsCl} \cdot 1/3(2\text{H}_3\text{O}^+\text{ClHCl}^-)$ ¹⁶ and the gas phase.¹⁷

The distribution of bending angles (Figure 3b) clearly shows a maximum at $\alpha = 180^\circ$, corresponding to a linear structure. These results show that the complex should be thought of as a $[\text{ClHCl}^-]$ molecule, rather than a hydrogen-bonded complex of the form $\text{Cl}^- \cdots \text{HCl}$, similar to that observed in solid $[\text{Me}_4\text{N}^+]\text{ClHCl}^-$.¹⁶ To conclude, the surrounding ions in the IL do not break the symmetry of the gas-phase anion.

The symmetry and linearity of ClHCl^- resemble those of FHF^- , which is present in a variety of ILs, like the highly conducting $[\text{NH}_4][\text{HF}_2]^{25}$ and $[\text{EMIF}][2.3\text{HF}]^{26}$ or superacidic mixtures such as $[\text{KF}-2\text{HF}]$. In the last two cases, FHF^- , and species containing more than one HF unit, coexist in dynamical equilibrium.^{27,28}

The coordination of ClHCl^- with its neighboring ions ($[\text{dmim}^+]$ and Cl^-), together with the number and strength of the hydrogen bonds it forms with the cation hydrogens, determine how tightly the molecule is held by its solvation shell. These interactions affect the mobility of the anion and thus its charge transport ability. Radial distribution functions ($g_{\text{ClH}}(r)$) between the Cl atoms in ClHCl^- and ring and methyl hydrogens are shown in Figure 4. These functions were averaged over the two equivalent chlorines that, taken separately, gave slightly different curves, thus contributing to the magnitude of the error bars. Up to a distance of 3.5 Å from a chlorine atom there are two ring hydrogen atoms and four hydrogens belonging to

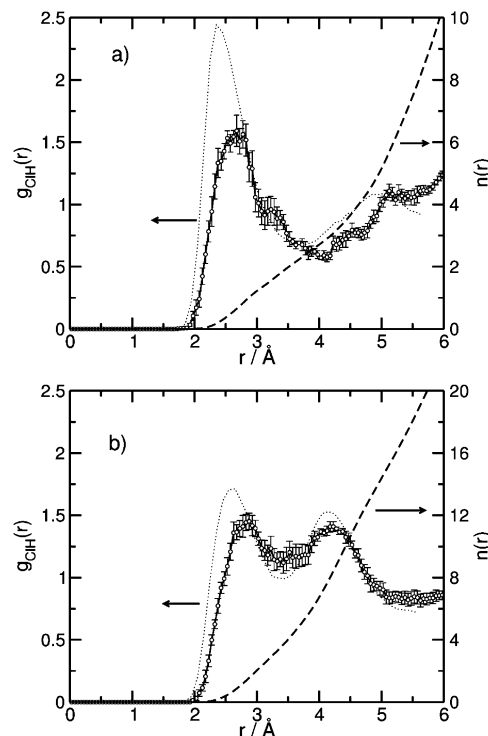


Figure 4. Radial distribution functions, $g_{\text{ClH}}(r)$: (a) between the Cl atoms in ClHCl^- and ring hydrogens and (b) between Cl atoms and methyl hydrogens. The corresponding coordination numbers are shown on the right axis. The dotted lines correspond to the equivalent Cl^- –H distributions in the pure liquid.¹⁰

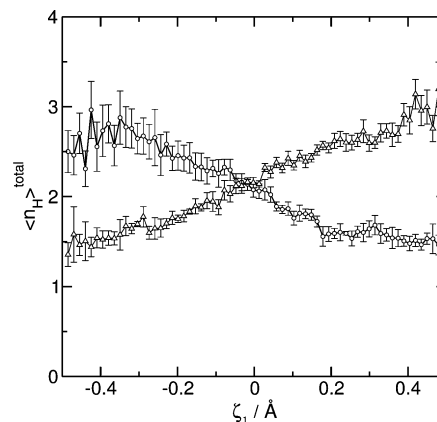


Figure 5. Number of hydrogen atoms up to a distance of 2.8 Å around each chlorine in ClHCl^- , as a function of the asymmetric stretching coordinate $\zeta_1 = l_1 - l_2$.

methyl groups. In both cases, the $g_{\text{ClH}}(r)$ values peak strongly at 2.5 Å, a distance only slightly larger than that corresponding to the maximum of the chloride–hydrogen distributions in the pure liquid (dotted lines).¹⁰ Although the former figures should be taken with care, due to the limited statistics provided by the simulations and the averaging over a single solute, the difference in the H-ring coordination numbers of ClHCl^- and Cl^- (3 for the pure liquid) arises from the fact that the former is a poorer hydrogen-bond acceptor. In fact, Trulove et al. have shown that there is no significant hydrogen-bonding between ClHCl^- and the imidazolium cation.²³

In line with the former arguments, the coordination of hydrogen atoms for each chlorine in ClHCl^- is markedly correlated with its asymmetric stretching. Figure 5 shows the number of hydrogen atoms up to a distance of 2.8 Å around each chlorine (Cl_1 and Cl_2), as a function of the asymmetric

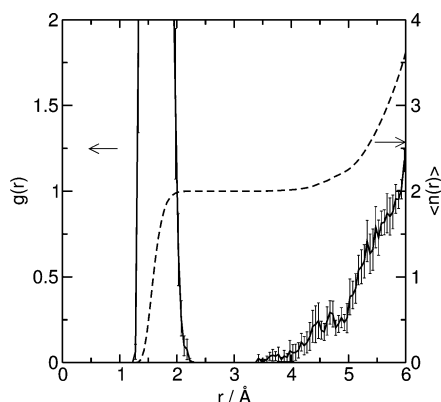


Figure 6. Radial distribution function and coordination number between the hydrogen atom in ClHCl^- and any chlorine atom in the simulation cell.

stretching coordinate, $\xi_1 = l_1 - l_2$. Clearly, when the molecule becomes asymmetric ($\xi_1 \neq 0$), the chlorine that moves away from the central hydrogen (for example, line with triangles for $\xi_1 > 0$) gains coordination, while the second (line with circles for $\xi_1 > 0$) loses. This behavior reflects a change in the partial charges on the chlorine atoms upon stretching, in such a way that the atom moving away gains negative charge while the second loses. However, this interaction with the solvent is not sufficient to cause symmetry breaking of the ClHCl^- ion.

With respect to the acidic hydrogen, the second nearest Cl^- appears beyond 4.0 Å, as can be observed in Figure 6, where the radial distribution function and coordination number between the hydrogen in ClHCl^- and any chlorine are shown. The first peak, that goes out of scale, accounts for the two flanking chlorines, while the rest of the distribution corresponds to the IL chloride ions. The position of the nearest anion beyond 5.5 Å (see the average coordination on the right axis of Figure 6), and the lack of a definite peak structure in the $g(r)$, clearly dismiss the existence of a stable complex of the form $\text{Cl}^- \cdots \text{ClHCl}^-$, as proposed in ref 24 and the observed in certain crystals.¹⁶ These nearest chlorides are however crucial for the proton exchange reaction to be described in the following section.

4. Proton Exchange Reaction

As shown in the former section, the proton remains associated in $[\text{dmim}][\text{Cl}]$. It stabilizes by forming two H–Cl bonds, whose strength determines the proton diffusion mechanism in the IL and thus its availability as a reactant or a catalyst.

There are two main possible diffusion mechanisms in the present system. A “shuttle” mechanism, where the acidic proton moves as an integral part of a ClHCl^- ion, its mobility being determined by the diffusion coefficient of the ion, and a “hopping” mechanism, involving the breaking of one of the H–Cl bonds and the formation of a new bond to one of the neighboring chlorides (see Figure 1). In general, the competitiveness of the two diffusion channels will depend on the strength of the different interactions compared with the temperature of the system.

In the absence of experimental information, we have to assume that both mechanisms are possible. The determination of the diffusion constant of ClHCl^- is computationally very demanding, because it requires long ab initio MD simulations. So, here we concentrate on the hopping mechanism.

To gain insight into the hopping process, umbrella sampling simulations were performed using the asymmetric stretching coordinate, $\xi_1 = l_1 - l_2$, as a reaction coordinate (see Figure

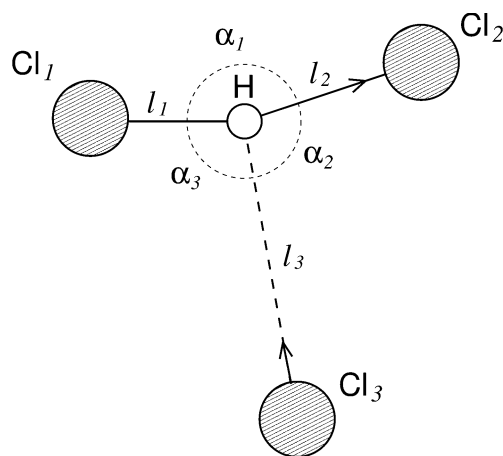


Figure 7. Old molecule is $\text{Cl}_1\text{HCl}_2^-$. Cl_3 enters and displaces Cl_2 forming a new molecule $\text{Cl}_1\text{HCl}_3^-$. ξ_1 is defined as $l_1 - l_2$. Note that if a distortion with negative ξ_1 occurs then Cl_1 and Cl_2 change roles.

7). For chemical reactions in solution, it is usually difficult to identify the best reaction coordinate, and in the present case, the exchange process may involve all the anions in the first solvation shell of ClHCl^- .

The asymmetric stretch would be the correct order parameter for a first-order mechanism, where the kinetic bottleneck is the formation of the complex $\text{Cl}^- \cdots \text{HCl}$. A second-order process involves the concerted departure and approach of the exchanging chlorides. If the proton is bonded to chlorine atoms 1 and 2 before the reaction and to atoms 1 and 3 after the reaction, such a reaction would be better described by the difference of H–Cl bond lengths between the entering and leaving chlorides, $\xi_2 = l_3 - l_2$.

Determining statistical averages in viscous liquids, such as the present ionic liquid, is difficult. The time scale accessible in ab initio MD simulations is far too short to explore a relevant region of phase space. For that reason, in the past, we have averaged over a set of initial conditions obtained from classical simulations.¹⁰ Here, this problem is aggravated because, for each biasing value of the reaction coordinate, a new equilibration of the system would be required. In the absence of such extensive calculations, the consequence is that the convergence of the free energy profile is poor, showing differences between the four independent systems studied and hysteresis upon reversing the sampling direction along ξ_1 . Such difficulties are reflected in Figure 8, where the free energy profile (symmetrized around the ordinate) is shown only for qualitative purposes. The average curve and the error bars were calculated from the eight curves that appear as dashed lines.

The lowest free energy curve in Figure 8 is acceptable, in the sense that the free energy after the proton-transfer event ($\xi_1 \approx 4$) coincides with the initial one. This should be so because the two configurations are equivalent from the thermodynamic point of view, since the only difference is that the HCl molecule is complexed with a different Cl^- in the liquid. Therefore, we take the barrier height corresponding to this curve, that is, $\Delta F_b^{\text{min}} = 0.3$ eV, as a lower bound for the true barrier. This trajectory, however, benefited from a favorable starting point, where one of the Cl^- ions in the liquid was already well-positioned for the proton-transfer event. The other curves clearly have suffered from more severe equilibration problems, as their free energies after the transfer event do not reach the original level. Nonequilibrated trajectories will tend to explore regions of higher internal energy. Consequently, we take the upmost curve in Figure 8, that is, $\Delta F_b^{\text{max}} = 0.8$ eV, as an upper bound

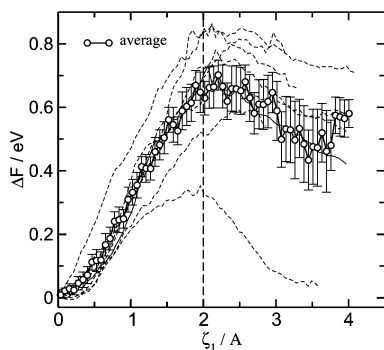


Figure 8. Free energy profiles along the reaction coordinate, ζ_1 , which is defined in the text. The average profile (circles with error bars) was calculated from four independent simulations exploring positive and negative values of ζ_1 . The negative branch of each profile was reflected around the ordinate leading to the eight curves (dashed lines) that appear in the plot. The dotted vertical line shows the estimated position of the transition state.

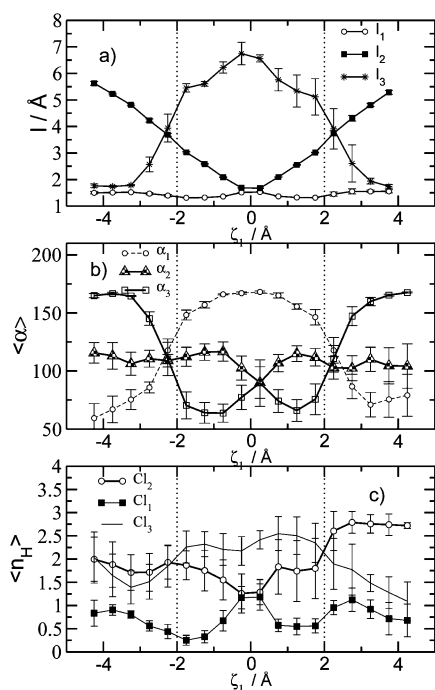


Figure 9. (a) Average value of l_1 , l_2 , and l_3 (see Figure 7 for their definition) as a function of ζ_1 . (b) Average angles between the H–Cl₁ and H–Cl₂ bonds (α_1), the H–Cl₂ and H–Cl₃ bonds (α_2), and the angle between H–Cl₁ and H–Cl₃ (α_3). (c) Number of ring hydrogen atoms in the vicinity of the chlorines involved in the reaction. The dotted vertical lines show the estimated position of the transition state. Error bars were calculated from four independent simulations.

for the free energy barrier. On the basis of the above considerations, we believe that the true barrier lies between 0.4 and 0.7 eV.

In variance with the free energy profile, the structural evolution of the reacting molecules exhibited a much more reproducible behavior. Figure 9a shows the average values of l_1 , l_2 , and l_3 (defined in Figure 7), as function of ζ_1 . At the stable configuration, $\zeta_1 \sim 0$ Å, the entering chlorine (Cl₃) is far from the acidic hydrogen, so that l_3 is large while l_1 and l_2 take their equilibrium values. Upon distortion of the ClHCl[−] ion, Cl₃ spontaneously approaches as the hydrogen atom gains positive charge. From the inspection of the free energy profile, the kinetic bottleneck seems to occur at $|\zeta_1| \sim 2$ Å (vertical lines in Figures 8 and 9), a point where $l_3 > l_2$ indicating that Cl₃ is still away from the dissociating complex Cl₂[−]⋯HCl₁.

Afterward, the leaving chlorine (Cl₂) moves out as Cl₃ and Cl₂ repel each other. As the reaction progresses, the H–Cl bond length to the chlorine atom which remains bonded, l_1 , first decreases slightly and then recovers its original value as the new molecule is formed. At this point, it is important to emphasize that the role of the Cl₁ and Cl₂ atoms has to be exchanged for negative values of ζ_1 .

Panel (b) of Figure 9 shows the average angles between the three H–Cl bonds, as a function of ζ_1 . α_1 is the angle between the bonds in the initial molecule (H–Cl₁ and H–Cl₂), α_2 the angle between the old and new bonds (H–Cl₃ and the H–Cl₂), while α_3 corresponds to the angle between the bonds in the final molecule (H–Cl₁ and H–Cl₃). For values of ζ_1 near zero, ClHCl[−] remains linear, showing an average bending of $\alpha_1 \sim 170^\circ$. It must be kept in mind that for a linear triatomic molecule the average bending differs from the most probable value, which is given by the maximum of the distribution (see Figure 3b). Even if the error bars on α_2 and α_3 are large, for values of ζ_1 between ± 2 Å, the entering chloride appears to attack ClHCl[−] roughly perpendicularly to its axis (angles between 60° and 120°). Starting from $\zeta_1 \sim 0$, and after a small drop, α_3 increases while α_1 decreases upon stretching, and the two curves cross at $|\zeta_1| \sim 2$ Å. At this point of ζ_1 , the angle between the entering and the leaving chlorides is around 115° . In the final state, α_3 reaches the equilibrium value of 170° as the exchange process is completed, while the leaving Cl[−] ends up perpendicular to the ClHCl[−] molecule ($\alpha_1 \sim 90^\circ$).

As shown in the previous section, the coordination of ClHCl[−] with the cation hydrogens (H₈, H₉, and H₁₀ in Figure 2) differs from that of Cl[−]. Therefore, the coordination numbers of Cl₃ and Cl₂ have to change during the reaction, introducing an important contribution to the activation free energy. Figure 9c shows the average number of ring hydrogens located within a radius of 3 Å around the chlorines participating in the reaction. This cutoff includes the first maximum of $g_{\text{ClH}}(r)$ at $\zeta_1 = 0$. The curves depict a clear qualitative trend, although the lack of symmetry with respect to $\zeta_1 = 0$ indicates the difficulty to converge the free energy profile within acceptable accuracy. For values of ζ_1 close to zero, the coordination of the leaving and the staying chlorines is the same and around 1.3 H atoms. Upon stretching, Cl₂ gains coordination as it turns into Cl[−], while the coordination of Cl₁ passes through a minimum and rises again. On the other hand, the entering chloride has a high H coordination when it is far from ClHCl[−] ($\zeta_1 \sim 0$) and decoordinates as the ion is incorporated into the new molecule. Once again, the curves for Cl₂ and Cl₃ cross at $|\zeta_1| \sim 2$, the plausible location of the transition state (dotted vertical lines). Due to the limited extent of the simulations, the solvation structure of the new ClHCl[−] ($\zeta_1 \sim \pm 4$) is not, as it should be, exactly the same as that of the original anion, at least for negative values of ζ_1 .

5. Conclusions

In the present work, we have studied the state of a single Brønsted acid molecule, HCl, in the ionic liquid [dmim][Cl]. Our DFT-based simulations show the formation of hydrogen dichloride, as a linear symmetric molecule, in the molten salt. These findings agree with the spectroscopic measurements of Trulove et al.²³ but differ from the observations of Trouw and Price.²⁴

The first solvation shell of ClHCl[−] is formed by cation hydrogens, belonging to both, imidazolium rings and the methyl groups. The corresponding coordination numbers are lower than those of Cl[−] in the pure liquid.¹⁰ The number of hydrogen atoms

solvating each chlorine correlates with the asymmetric distortion of the anion, as their effective charges vary with this coordinate. For the most stretched configurations, that can be thought of as complexes of the form $\text{Cl}^- \cdots \text{HCl}$, the chlorine that leaves the complex gains coordination while the second loses. However, the stabilization of the distorted form by solvation is not sufficient to cause symmetry breaking, unlike I_3^- in water.²⁹ The formation of ion pairs of the form $\text{Cl}^- \cdots \text{ClHCl}^-$, as proposed in ref 24 to explain a possible asymmetry of ClHCl^- , is not supported by the present results.

We have discussed a proton exchange reaction, where the anions (Cl^-) serve as proton donor and acceptor sites. Due to an extremely time-consuming equilibration, it was not feasible to obtain a free energy profile free from systematic errors. However, our data provided a rough estimate of the activation barrier of 0.4–0.7 eV. At variance with the energetic, the structural evolution of the reaction complex and its solvation shell along the reaction coordinate showed a more reproducible behavior. When ClHCl^- is asymmetrically stretched, one of the neighboring chlorides approaches the hydrogen atom perpendicularly to the axis of the $\text{Cl}^- \cdots \text{HCl}$ complex. The formation of this hydrogen-bonded complex seems to be the kinetic bottleneck and occurs at $|\xi_1| \sim 2 \text{ \AA}$. The exchange process ends with the expulsion of the leaving chloride and the formation of a new ClHCl^- molecule.

This work is a first step toward understanding the transport mechanisms available to protons in room-temperature molten salts.

Acknowledgment. This work was funded by EPSRC, Grants GR/S41562 and EP/D029538/1. R.M.L.B. thanks the Leverhulm Trust for an Emeritus Fellowship. The computations reported in this work have been partially carried out using the facilities provided by the HPCx Consortium, U.K.

References and Notes

(1) Rogers, R. D.; Seddon, K. R.; Volkov, S. *Green Industrial Applications of Ionic Liquids*; NATO Science Series; Kluwer Academic Publishers: Boston, MA, 2002.

- (2) Wasserscheid, P.; Welton, T., Eds. *Ionic Liquids in Synthesis*; Wiley VCH: Weinheim, Germany, 2002.
- (3) Angell, C. A.; Xu, W.; Yoshizawa, M.; Belieres, J. P. In *International Symposium on Ionic Liquid*; Carry Le Rouet, France, 2003; pp 389–398.
- (4) Susan, M. A.; Noda, A.; Mitsushima, S.; Watanabe, M. *Chem. Commun.* **2003**, 8, 938–939.
- (5) Yoshizawa, M.; Xu, W.; Angell, A. J. *Am. Chem. Soc.* **2003**, 125, 15411–15419.
- (6) Noda, A.; Susan, M. A.; Kudo, K.; Mitsushima, S.; Mitsushima, S.; Hayamizu, K.; Watanabe, M. *J. Phys. Chem. B* **2003**, 107, 4024–4033.
- (7) Soler, J. M.; Artacho, E.; Gale, J.; García, A.; Junquera, J.; Ordejón, P.; Sánchez-Portal, D. *J. Phys.: Condens. Matter* **2002**, 14, 2745–2779.
- (8) Perdew, J.; Burke, K.; Ernzerhof, M. *Phys. Rev. Lett.* **1996**, 77, 3865–3868.
- (9) Troullier, N.; Martins, J. L. *Phys. Rev. B* **1991**, 43, 1993.
- (10) Del Pópolo, M. G.; Lynden-Bell, R. M.; Kohanoff, J. *J. Phys. Chem. B* **2005**, 109, 5895–5902.
- (11) Allen, M.; Tildesley, D. *Computer Simulation of Liquids*; Clarendon: Oxford, U.K., 1987.
- (12) Canongia Lopes, J. N.; Deschamps, J.; Padua, A. A. H. *J. Phys. Chem. B* **2004**, 108, 2038.
- (13) Lide, D. R., Ed. *CRC Handbook of Chemistry and Physics*, 83rd ed.; CRC Press: Boca Raton, FL, 2003.
- (14) Ludman, C. J.; Waddington, T. C.; Salthouse, J. A.; Lynch, R. J.; Smith, J. A. S. *Chem. Commun.* **1970**, 227, 405.
- (15) Shuppert, J. W.; Angell, A. J. *Chem. Phys.* **1977**, 67, 3050–3056.
- (16) Emsley, J. *Chem. Soc. Rev.* **1980**, 1, 91–124.
- (17) Kawaguchi, K. *J. Chem. Phys.* **1988**, 88, 4186–4189.
- (18) Thomson, C.; Clark, D. T.; Waddington, T. C.; Jenkins, H. D. B. *J. Chem. Soc., Faraday Trans.* **1975**, 2, 1942–1947.
- (19) Del Bene, J. E.; Jordan, M. J. *Spectrochim. Acta, Part A* **1999**, 55, 7197–729.
- (20) Pimentel, G. C.; McClellan, A. L. *Annu. Rev. Phys. Chem.* **1971**, 22, 347–385.
- (21) Pine, A. S.; Howard, B. J. *J. Chem. Phys.* **1986**, 84, 590–596.
- (22) Trulove, P. C.; Sukumaran, D. K.; Osteryoung, R. A. *Inorg. Chem.* **1993**, 32, 4396–4401.
- (23) Trulove, P. C.; Osteryoung, R. A. *Inorg. Chem.* **1992**, 31, 3980–3985.
- (24) Trouw, F. R.; Price, D. L. *Annu. Rev. Phys. Chem.* **1999**, 50, 571–601.
- (25) Xu, W.; Angell, A. *Science* **2003**, 302, 422–425.
- (26) Hagiwara, R.; Hirashige, T.; Tsuda, T.; Ito, Y. *J. Electrochem. Soc.* **2002**, 149, D1–D6.
- (27) von Rosenvinge, T.; Parrinello, M.; Klein, M. L. *J. Chem. Phys.* **1997**, 107, 8012–8019.
- (28) Simon, C.; Cartailier, T.; Turq, P. *J. Chem. Phys.* **2002**, 117, 3772–3779.
- (29) Zhang, F. S.; Lynden-Bell, R. M. *Phys. Rev. Lett.* **2003**, 90, 185505.